Analysis of a Wet Surface Finned-tube Evaporator of an Air Source Heat Pump

Young-Jin Baik*, Young-Soo Chang* and Youngil Kim*

Key words: Heat and mass transfer, Finned-tube, Evaporator, Wet surface, Heat pump

Abstract

In this study, in-situ performance test of a wet surface finned-tube evaporator of an air source heat pump which has a rating capacity of 20 RT is carried out. Since test conditions, such as indoor and outdoor air conditions cannot be controlled to satisfy the standard test conditions, experiments are done with the inlet air conditions as they exist. From the experimental data, air side heat and mass transfer coefficients were calculated by the well known heat and mass transfer analogy and tube-by-tube method. Since current procedure underpredicted the experimental sensible heat factor (SHF), a proper empirical parameter was introduced to predict the experimental data with satisfactory results. This study provides the method of evaluating the heat and mass transfer coefficients of a wet surface finned-tube evaporator of which in-situ performance test is necessary.

Nomenclature

A : area [m^2]
$\hat{i}$: enthalpy variation over temperature variation of saturated moist air [kJ/kg · K]
Bo : boiling number
c_f : friction coefficient
Co : convection number
c_p : specific heat [kJ/kg · K]
d : diameter [m]
D_{AB} : diffusion coefficient [m^2/s]
i : enthalpy [kJ/kg]
i^* : enthalpy of saturated moist air [kJ/kg]
FP : fin pitch [m]
G : mass flux [$kg/m^2 \cdot s$]
h : heat transfer coefficient [$kW/m^2 \cdot K$]
h_m : mass transfer coefficient [$kg/m^2 \cdot s$]
I : tube expansion interference[15] [m]
i_{fg} : latent heat of evaporation [kJ/kg]
Le : Lewis number, α/D_{AB}
Le' : experimental constant, Eq. (10)
NTU : number of transfer unit
P : pressure [kPa]
Q : heat transfer rate [kW]
$\dot{q}$: heat flux [kW/m^2]
SHF : sensible heat factor [%]

* Thermal/Fluids Control Research Center, Korea Institute of Science and Technology, 39-1 Hawolgok-dong, Seongbuk-gu, Seoul 136-791, Korea

T : temperature [K]
t_f : fin thickness [m]
U : overall heat transfer coefficient [$kW/m^2 \cdot K$]
$\dot{v}$: volumetric flow rate [m^3/s]
v_{front} : frontal velocity of inlet air [m/s]
w : humidity ratio [kg/kg_{DA}]
w^* : humidity ratio of saturated moist air [kg/kg_{DA}]
x : quality

Greek symbols

α : thermal diffusivity [m^2/s]
ε : effectiveness
η_s : fin efficiency
ρ : density [kg/m^3]
ϕ : fin geometric parameter[16]

Subscripts

a : air side
c : contact
cond : condenser
eva : evaporator
f : fin
i : inner side
lat : latent
o : outer side
OA : outdoor air
out : outdoor air
r : refrigerant side
RA : return air
SA : supply air
sen : sensible

1. Introduction

Due to recent concern about the depletion of natural resources and environmental problem, considerable attention on energy saving has grown up and a great number of research projects related to this topic have been carried out. More recently, ESCO (Energy Service Company) has been established by the Government for promoting energy saving projects effectively. ESCO has a wide range of business, but among them air-conditioning field has been an important issue because in general, energy consumed by air-conditioning system (including ventilation and sanitary facilities) accounts for about 47% of the total energy consumption, compared to lighting 24% and others 29%. In order to understand the actual status of building energy consumption, in-situ diagnosis method of air-conditioning system needs to be developed.

Air-conditioning system consists of chiller, AHU (air handling unit) and other facilities. Among them, heat exchanger diagnosis can be regarded as an essential process for the diagnosis of total system performance. Heat exchanger performance can be presented by overall heat transfer coefficient and pressure drop. One of the most important factors when analyzing heat exchangers is the air-side heat transfer coefficient, which should be measured for the accurate diagnosis and performance prediction of the total system. An air-side mass transfer coefficient, which accounts for dehumidifying performance, is also an important factor especially for the cooling coil.

A finned-tube type cross-flow heat exchanger is widely used for air-conditioning purpose and is composed of circular copper tubes and aluminum fins, which are tightly assembled together by mechanical enlarging process of tubes. Refrigerant flows in the copper tubes and air flows perpendicularly to the refrigerant flow through the fins. A lot of researches on the performance test and analysis of a finned-tube type cross-flow heat exchanger have been carried out by many researchers. Park et al.[1] investigated the performance variations of finned-tube type cross-flow heat exchanger with its design variables and conditions and Yun

and Lee[2] studied characteristics of finned-tube heat exchangers with various interrupted surfaces experimentally. Hiller and Glicksman[3] and Fischer and Rice[4] divided heat exchanger into three parts according to the refrigerant states and analyzed them by ε-NTU method. Domanski[5] established tube-by-tube method with the assumption of refrigerant-side mixed and air-side unmixed.

Analysis of heat exchanger becomes more complicated if heat and mass transfer occur simultaneously such as cooling coil or direct feed evaporator. Han and Kim,[6] and McQuiston and Parker[7] tried to analyze mass transfer phenomenon by classical heat transfer relation and analogy between heat and mass transfer. Kim et al.[8] investigated wet surface performance of heat exchangers with slit-wavy fin experimentally. Yoon et al.[9,10] also investigated wet surface evaporator performance with tube-by-tube method[5] and testified their modelling with their experimental results. They also emphasized that there is no doubt about general dry surface modelling, but for wet surface, of which temperature is lower than the dew point temperature of the air, with its complicated dehumidification process, no irrefutable modelling exists. Performance of heat exchangers installed in the field may be inferior to those in the laboratory because of contamination such as dust.

In this study, air side heat and mass transfer coefficients were calculated by conventional method proposed by above-mentioned researchers with in-situ performance test results of an air source heat pump. Also, conventional methods based on the theoretical analysis and various assumptions were investigated whether they could be used to analyze the heat exchangers operating in the field.

2. Experimental apparatus and procedures

The system investigated in this study is an air source heat pump that has a rated cooling capacity of 20 RT (or 70 kW). The system has two 7.5 kW hermetic reciprocating compressors and uses HCFC-22 as the working fluid. The evaporator is a 6-row 18-tubes with 18-circuits finned-tube type cross-flow heat exchanger. It is composed of copper tube with inner and outer diameters of 8.52 mm and 9.52 mm respectively and corrugated aluminum fin with 3.2 mm fin pitch. The condenser is 5-row 22-tubes with 22-circuits, which is composed of the same tube and fin as the evaporator except 2.1 mm fin pitch. Thermostatic expansion valves, accumulators, filter dryers, suction strainers and sight glasses are also parts of the refrigerant line. A 7.5 kW airfoil fan with capacity of 180 CMM at 90 mmAq static pressure is used for the supply. Temperatures, humidities, pressures and flow rates are measured for the calculation of heat and mass transfer coefficients. Temperatures are measured by T type thermocouples with ± 0.1℃ accuracy. Humidity transmitters with accuracy of $\pm 2\%$ are used. Condenser and evaporator outlet pressures are measured by strain gauge type pressure transducers with accuracy of $\pm 0.1\%$. A turbine type flow meter with $\pm 0.5\%$ accuracy is used to measure refrigerant volumetric flow rate. Pitot tube and micro-manometer with accuracy of $\pm 0.1\%$ are used for air velocity measurement. Volumetric flow rate of air in the rectangular duct is determined by center air velocity and predetermined relation between center air velocity and average air velocity. For fully developed flow in the rectangular duct, relation between center air velocity and average air velocity can be obtained by method of Hartnett et al.[11] Since practical duct flows are not always fully developed, average air velocity measurement in practice requires many measuring points. For a rectangular duct, 16~64 measuring points are proposed by T.A.B. Standard for HVAC applications[12] and thus 16 points are used in this study. All instruments

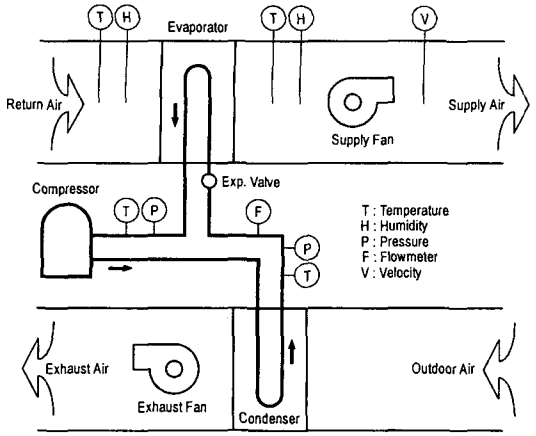

Fig. 1 Schematic diagram of an experimental apparatus.

are scanned by data acquisition system and transferred to a personal computer through GPIB and NI Labview program. Schematic diagram of an experimental heat pump is shown in Fig. 1.

Since experimental heat pump was installed in the field, experimental conditions could not be controlled and experiments were done with inlet air conditions as they existed. Experimental data were collected every 2 second and if all temperature changes were within ±0.2℃ for 20 minutes, these were regarded as steady state condition. Experiments were carried out from June 19, 2000 to June 28, 2000 and among lots of data, 15 sets were used to calculate heat and mass transfer coefficients. Experimental conditions are shown in Table 1. The mean heat balance error in the evaporator was 9.2% and average value between refrigerant

Table 1 Experimental condition

T_{OA} [℃]	21.8~31.8
T_{RA} [℃]	21.4~23.2
RH_{RA} [%]	54.3~72.0
P_{eva} [kPa]	464~503
P_{cond} [kPa]	1524~1951
$\dot{V}_{SA}$ [m^3/s]	2.57~2.61
v_{front} [m/s]	1.82~1.84
SHF [%]	65~81

heat gain and air heat loss, which was regarded as heat transfer rate, was used to calculate heat and mass transfer coefficients.

3. Wet surface modelling

Although a lot of analysis methods are available, tube-by-tube method is widely used to analyze finned-tube heat exchanger due to its accuracy and simplicity. More accurate analysis can be performed by finite element method, but its effective advantage is not significant because it requires much time and additional assumptions.[9] Sensible heat transfer and latent heat transfer occur simultaneously on wet surface, of which temperature is lower than the dew point temperature of the air. The total heat transfer rate is given by Eq. (1).

$$Q = h_a A_a \eta_s dT + h_m i_{fg} A_a \eta_s dw \tag{1}$$

A relation between heat and mass transfer coefficients can be presented as Eq. (2) by heat and mass transfer analogy.

$$\frac{h_a}{c_{pa} h_m} = \mathrm{Le}^{2/3} \tag{2}$$

Assuming Le=1 for moist air, from Eq. (1) and Eq. (2), total heat transfer rate on the wet surface can be presented as Eq. (3). Also, assuming no thermal resistance is caused by the tube wall, condensate and fouling, overall heat transfer coefficient and heat transfer rate are given in Eq. (4) and Eq. (5)[9] respectively.

$$Q = \frac{h_a}{c_{pa}} A_a \eta_s (i_a - i_o^*) \tag{3}$$

$$\frac{1}{U'A} = \frac{\hat{i}}{h_i A_i} + \frac{\hat{i}}{h_c A_c} + \frac{c_{pa}}{h_a A_a \eta_s} \tag{4}$$

$$Q = U'A(i_a - i_r^*) \tag{5}$$

where $\hat{i}$ in Eq. (4) is enthalpy variation over

temperature variation of saturated moist air, h_i is refrigerant side heat transfer coefficient which can be calculated by Eq. (6) proposed by Kandlikar.[13]

$$h_i = h_l\left[C_1 \mathrm{Co}^{C_2}(25\,\mathrm{Fr}_{le})^{C_5} + C_3\,\mathrm{Bo}^{C_4} F_K\right] \quad (6)$$

In Eq. (6), $h_l = 0.023\left(\frac{k_l}{d}\right)\mathrm{Re}_l^{0.8}\,\mathrm{Pr}_l^{0.4}$, $\mathrm{Co} = \left(\frac{1-x}{x}\right)^{0.8}\left(\frac{\rho_v}{\rho_l}\right)^{0.5}$, $\mathrm{Bo} = \frac{\dot{q}}{G \cdot i_{fg}}$, $\mathrm{Fr}_{le} = \frac{G^2}{\rho_l^2 g d}$, F_K and $C_{1,2,3,4,5}$ are constants. For a superheated region, h_i can be calculated by Eq. (7) proposed by Gnielinski.[14] Heat transfer coefficient h_c given by Eq. (8)[15] denotes contact resistance between fin collar and tube.

$$h_i = \left(\frac{k}{d}\right)\frac{(\mathrm{Re}-1000)\,\mathrm{Pr}\,(c_f/2)}{1.0+12.7\sqrt{c_f/2}\,(\mathrm{Pr}^{2/3}-1.0)} \quad (7)$$

$$h_c = 5.7\exp\left[7.83 + 2.9\left(\frac{0.0254 I \cdot d_i}{FP \cdot d_o}\right)^{0.75}\left(\frac{t_f}{FP}\right)^{1.25}\right] \quad (8)$$

where η_s is fin efficiency for wet surface and can be presented as Eq. (9)[9] from Schmidt[16] approximation and Threlkeld[17] theorem.

$$\eta_s = 1 - \frac{A_{\mathrm{fin}}}{A_a}\left(1 - \frac{\tanh\left(\sqrt{\frac{2\hat{a}h_a}{c_{pa}k_f t_f}}\,d_o\frac{\phi}{2}\right)}{\sqrt{\frac{2\hat{a}h_a}{c_{pa}k_f t_f}}\,d_o\frac{\phi}{2}}\right) \quad (9)$$

Once heat transfer rate is calculated from experiments, heat and mass transfer coefficients can be calculated by Eq. (1)~(9) and tube-by-tube method with assumptions of all finned surface condensation occurrence if tube outer wall temperature is lower than the dew point temperature, no air mixing among steps and complete condensate drain.[9]

The steps for the calculation of heat and mass transfer coefficients from experimental data are as follows. First, assume heat transfer coefficient and then calculate mass transfer coefficient. Through the air-side first row single-tube cross flow heat exchanger analysis, inlet air condition for second row and outlet refrigerant condition can be calculated. After all calculations for each row as mentioned above are done, evaporator inlet refrigerant condition can be obtained. If this condition is different from experimental result, reassume heat transfer coefficient and the above process is repeated. Fig. 2 shows evaporator simulation process mentioned above.

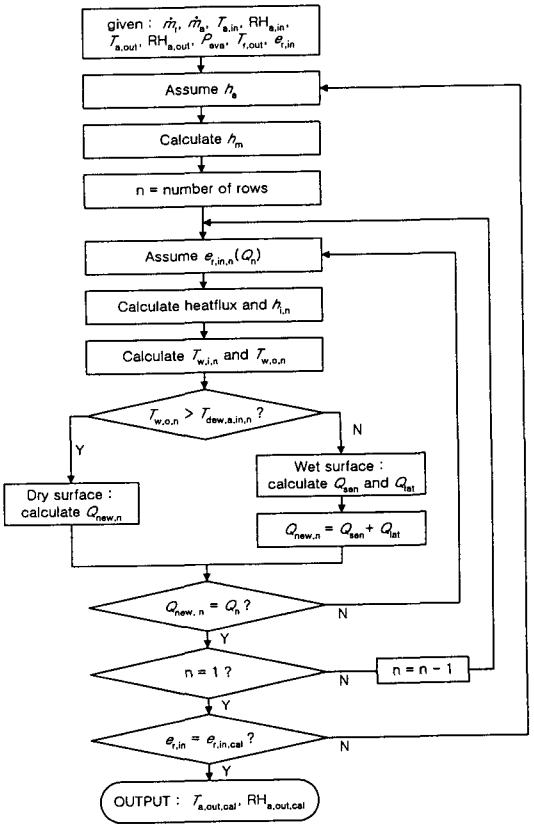

Fig. 2 Evaporator simulation program.

4. Results and discussions

Fig. 3 shows the average ratio of heat and mass transfer coefficients for 15 experimental

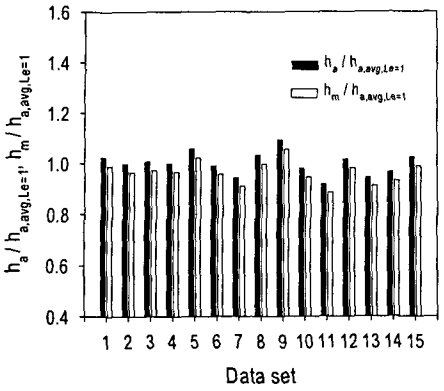

Fig. 3 Heat and mass transfer coefficients (Le=1).

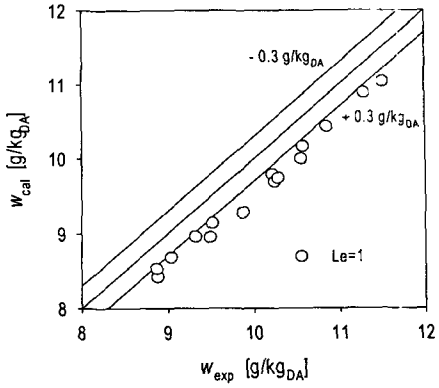

Fig. 5 Comparison of experimental $w_{eva,out}$ with predicted $w_{eva,out}$.

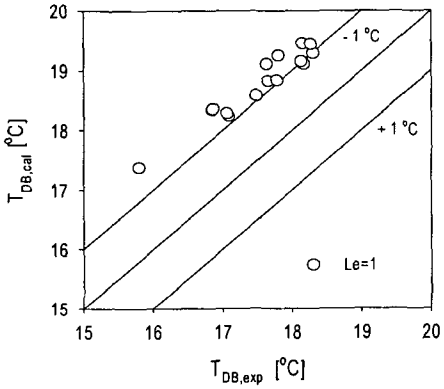

Fig. 4 Comparison of experimental $T_{eva,out}$ with predicted $T_{eva,out}$.

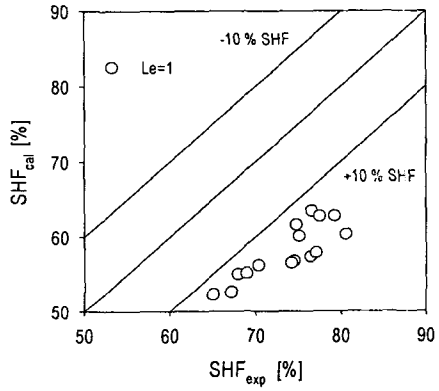

Fig. 6 Comparison of experimental SHF with predicted SHF.

data set. Figs. 4, 5 and 6 show calculated evaporator outlet air temperatures, humidities and SHFs (sensible heat factors) respectively. Fig. 3 indicates that heat and mass transfer coefficients have small variation, since the experiments were carried out for almost the same air flow rate, which is a typical situation in the field. For all data, simulation results over-predicted latent heat transfer and under-predicted sensible heat transfer according to Fig. 4, 5 and 6, and it seems that conventional analysis method based on many assumptions can not simulate field characteristics which is significantly different from ideal conditions.

The factors for causing deviations of field performance tests which result in higher SHF than calculated SHF with assumption of ideal condition are as followings. First, contamination can be a primary factor. The experimental heat pump installed in the field has been operated for many years. Dust and leaves which are attached to the surface of the heat exchanger, can interfere with heat and mass transfer. If they disturb smooth condensate drain on the heat exchanger surface, actual latent heat transfer can be reduced and will yield lower SHF than predicted values obtained through theoretical analysis. Maldistribution of refrigerant in the heat exchanger also can be a problem. No problem occurs if all tubes have enough refrigerant flow. But, once a circuit lacks refrigerant flow, its evaporating temperature rise ra-

pidly to yield droplet carry over, which results in condensate accumulation on the surface and influx to the supply air.[18]

But it is very difficult to investigate aforementioned issues in the field. As mentioned above, heat pump investigated experimentally in this study has characteristics of high SHF. To solve this problem, all parameters that are related to the calculation of SHF are investigated. Empirical constant are then introduced for better estimation. With definition of experimental constant Le′ as Eq. (10) and X as Eq. (11), heat transfer rate can be approximated as Eq. (12) and overall heat transfer coefficient and total transfer rate can be presented as Eq. (13) and Eq. (14), respectively. According to Eq. (12) and Eq. (13), heat transfer rate is proportional to the sum of enthalpy difference and X calculated by Eq. (11). For the same heat transfer coefficient, higher Le′ results in lower X and higher thermal resistance and thus lower heat transfer rate.

$$\mathrm{Le}' = \frac{h_a}{c_{pa} h_m} \tag{10}$$

$$X = \frac{i_{fg}(w_a - w_o^*)(1 - \mathrm{Le}')}{\mathrm{Le}'} \tag{11}$$

$$Q \fallingdotseq \frac{h_a}{c_{pa}} A_a \eta_s [(i_a - i_o^*) + X] \tag{12}$$

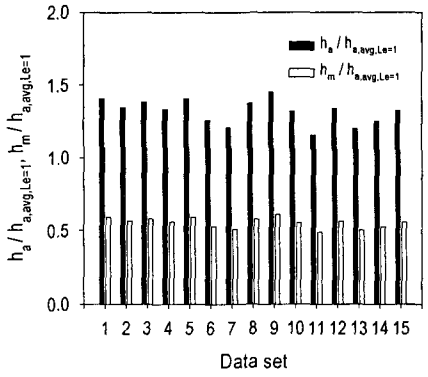

Fig. 7 Heat and mass transfer coefficients (Le′=2.3).

$$\frac{1}{U''A} = \frac{1}{U'A} - \frac{X}{\frac{h_a A_a \eta_s}{c_{pa}}[(i_a - i_o^*) + X]} \tag{13}$$

$$Q = U''A(i_a - i_r^*) \tag{14}$$

Each data needs a different Le′ value for the exact prediction of outlet air temperature, humidity and SHF. By curve-fitting the experimental data, Le′=2.3 shows acceptable results for all data. Fig. 7 shows heat and mass transfer coefficients calculated by Eq. (10)~(14) with Le′=2.3. The results are divided by the average heat transfer coefficient with Le=1. Fig. 8, 9 and 10 show comparison of calculated evaporator outlet air temperatures, humidities and SHFs with experimental results. Fig. 7 indi-

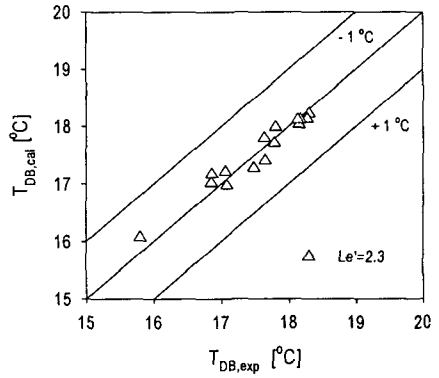

Fig. 8 Comparison of experimental $T_{eva,out}$ with predicted $T_{eva,out}$.

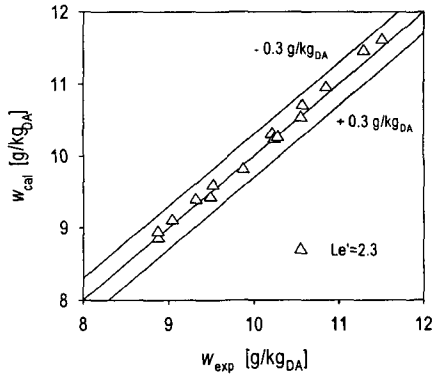

Fig. 9 Comparison of experimental $w_{eva,out}$ with predicted $w_{eva,out}$.

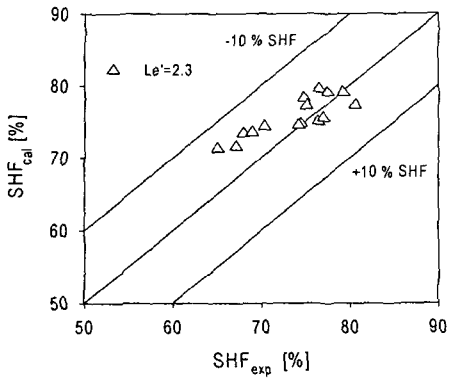

Fig. 10 Comparison of experimental SHF with predicted SHF.

cates 30% increase in heat transfer coefficients and 40% decrease in mass transfer coefficients in comparison with Fig. 3. With the new method, the field characteristics are reflected well. Prediction of outlet air conditions are also improved as shown in Fig. 8, 9 and 10.

5. Conclusions

In case of heat and mass transfer coefficient calculations from in-situ performance test results, the field characteristics should be implemented for proper evaluation. In this study, experimental constants Le′ and X were introduced and satisfactory results are acquired. Extensive studies, however are still required for complete explanation of abstruse field characteristics.

References

1. Park, H. Y., Park, D. K. and Lee, K. S., 1989, Modeling of fin-tube heat exchanger, Transactions of the Korean Society of Mechanical Engineers, Vol. 13, No. 5, pp. 952-961.
2. Yun, J. Y. and Lee, K. S., 1996, Heat transfer characteristics of fin and tube heat exchangers with various interrupted surfaces for air conditioning application, Transactions of the Korean Society of Mechanical Engineers B, Vol. 20, No. 12, pp. 3938-3948.
3. Hiller, C. C. and Glicksman, L. R., 1976, Improving heat pump performance via compressor capacity control-analysis and test, MIT Energy Lab.
4. Fischer, S. K. and Rice, C. K., 1980, The Oak Ridge heat pump models: I. A steady-state computer design model for air-to-air heat pumps, ORNL/CON-80/R1, Oak Ridge National Lab.
5. Domanski, P. A., 1989, EVSIM-An evaporator simulation model accounting for refrigerant and one dimensional air distribution, NISTIR 89-4133, U. S. Dept. of Commerce, NIST, Maryland 20899.
6. Han, C. S. and Kim, K. W., 1996, The air side heat transfer coefficient on the wetted surface of fin and tube heat exchanger, Air-Conditioning and Refrigeration Engineering, SAREK, Vol. 25, No. 2, pp. 161-173.
7. McQuiston, F. C. and Parker, J. D., 1997, Heating, ventilating, and air conditioning: analysis and design, 4th ed., John Wiley & Sons, Inc., pp. 543-547.
8. Kim, N. H., Kim, J. S., Cho, J. P., Yun, J. H., Peck, J. H., Lee, S. G., Nam, S. B. and Kwon, H. J., 1997, Wet surface performance test of fin-tube heat exchangers with slit-wavy fin, Korean J. of Air-Conditioning and Refrigeration Engineering, Vol. 9, No. 2, pp. 153-162.
9. Yoon, B., Yoo, K. C., Park, H. Y. and Kim, Y. S., 1996, Modeling of cross-flow fin-tube evaporator, The Korean Society of Mechanical Engineers Symposium Series: Thermal and Fluid Engineering Section, pp. 73-81.
10. Yoon, B., Park, H. Y., Yoo, K. C. and Kim, Y. C., 1999, Air-conditioner cycle simulation using tube-by-tube method, Korean Journal of Air-Conditioning and Refrigeration Engineering, Vol. 11, No. 4, pp. 499-510.
11. Hartnett, J. P., Koh, J. C. Y. and Mccomas, S. T., 1962, A Comparison of predicted and measured friction factors for turbulent flow

through rectangular ducts, Trans. ASME J. Heat Transfer, pp. 82-88.

12. SAREK, 1999, T.A.B. Standard for HVAC applications.
13. Kandlikar, S. G., 1990, A general correlation for saturated two-phase boiling heat transfer inside horizontal and vertical tubes, Trans. ASME J. Heat Transfer, Vol. 112, pp. 219-228.
14. Gnielinski, V., 1976, New equations for heat and mass transfer in turbulent pipe and channel flow, International Chemical Engineering, Vol. 16, No. 2, pp. 359-368.
15. Sheffield, J. W., Wood, R. A. and Sauer, Jr., H. J., 1989, Experimental investigation of thermal conductance of finned tube contacts, Experimental Thermal and Fluid Science, Vol. 2, pp. 107-121.
16. Schmidt, T. E., 1949, Heat transfer calculations for extended surface, Journal of the ASRE, Refrigerating Engineering, Vol. 4, pp. 351-357.
17. Threlkeld, J. L., 1970, Thermal environmental engineering, Prentice-Hall, New York, pp. 257-259.
18. Hwang, Y. J., 2000, The optimum design of heat pump system with refrigerant distributor, The Society of Air-Conditioning and Refrigerating Engineers of Korea Symposium Series: Refrigeration Section, pp. 93-99.